# Study of scattering and radiative properties of complex soot aggregates

**Chengxin Lei (类成新)* and Dongtai Feng (冯东太)**

*School of Science, Shandong University of Technology, Zibo 255049, China*

**Corresponding author: xdpostgraduate@163.com*

Received December 27, 2011; accepted Feburary 24, 2012; posted online June 20, 2012

The discrete dipole approximation (DDA) method is used to calculate the scattering matrix elements and optical cross-sections for a wide variety of complex soot aggregates in random orientation at a visible wavelength of 0.628 $\mu$m. The effects of the material composition and the size of the larger particle that is in touch with soot cluster on scattering and radiative properties of complex soot aggregates are analyzed. It is shown that the material composition and the size of the larger particle can strongly influence or even dominate the overall scattering and radiative properties of the aggregates.

*OCIS codes:* 290.2200, 290.4210, 290.5850.
*doi: 10.3788/COL201210.S12901.*

Soot aggregates, well known as air pollutants, are primarily produced by imperfect combustion of fossil fuels and biomass burning. Knowledge of the scattering properties of soot aggregates is essential in a variety of applications such as optical diagnostics for industrial aerosol processes and combustion[1], environmental issues (visibility and haze problems), remote sensing[2], and astrophysical phenomena involving the effect of interstellar grains on light propagation and scattering. In the realm of terrestrial atmospheric physics, soot aggregates are perhaps the most important particulate absorber in the troposphere that absorb short-wave radiation from the sun, heat the air, and contribute to global warming[3,4]. Moreover, the effects of scattering and absorbing of soot aerosol on atmosphere radiation lead to the radiative properties of soot aerosol playing a significant role in infrared radiation transfer in atmosphere, as well as in remote atmospheric sensing and climate predictions[5−7]. Despite significant recent progresses in theory, model simulations, and measurements, the degree of quantitative understanding of the direct and indirect radiative forcing caused by carbonaceous aerosols remains limited[8], in part because of the complicated morphology of soot aerosols[9] and their tendency to mix with other aerosol species and act as cloud condensation nuclei.

It is well known that dry soot particles tend to exist in the form of clusters potentially consisting of hundreds of tiny monomers. It was demonstrated by Lei *et al.*[10−12] that the effects of aggregation, fractal morphology, and refractive index on the integral extinction, scattering, and absorption properties of soot aerosols could be quite significant. Those results suggest that the cluster structure of soot aerosols must be explicitly taken into account in remote sensing and radiation balance applications.

It has also been demonstrated that dry soot clusters may tend to aggregate with relatively large sulfate or dust particles. Even more complex semi-external aggregates consisting of more than two chemical components have often been encountered in various field campaigns. Therefore, the objective of this letter is to compute and analyze the scattering and radiative properties of these specific types of complex aerosols.

Carbonaceous soot particles frequently exist in the form of clusters of small, nearly spherical monomers (spherules). It has been demonstrated that the overall morphology of a dry soot aerosol is well represented by a fractal cluster described by the following statistical scaling law[13]:

$$N = k_{\mathrm{f}} \left( \frac{R_{\mathrm{g}}}{a} \right)^{D_{\mathrm{f}}}, \tag{1}$$

where $a$ is the monomer mean radius, $k_{\mathrm{f}}$ is the fractal prefactor, $D_{\mathrm{f}}$ is the fractal dimension, $N$ is the number of monomers in the cluster, and $R_{\mathrm{g}}$, called the radius of gyration, is a measure of the overall cluster radius, and is defined by

$$R_{\mathrm{g}}^2 = \frac{1}{N} \sum_{i=1}^{N} r_i^2, \tag{2}$$

where $r_i$ is the distance from center of sphere $i$ to the center of mass of aggregate. The fractal aggregate simulation was numerically generated using the cluster–cluster aggregation algorithm. The detailed description of the algorithms can be found in Ref. [14].

In this letter, the discrete dipole approximation (DDA) method is used to calculate the scattering and radiative properties of the numerically generated fractal complex aggregates in random orientation. The DDA is a general technique for calculating scattering and absorption of electromagnetic radiation by targets of arbitrary geometry and composition. The DDA was first proposed by Purcell *et al.*[15], who replaced the scatterer by a set of point dipoles. These dipoles interact with each other and the incident field, giving rise to a system of linear equations, which is solved to obtain dipole polarizations. All the measured scattering quantities can be obtained from these polarizations. The DDA was further developed by Draine *et al.*[16−18]. The key single-scattering characteristics of randomly oriented particles are the orientation-averaged scattering cross-sections $C_{\mathrm{sca}}$, extinction cross-sections $C_{\mathrm{ext}}$, and the elements of the normalized scattering matrix $\mathbf{S}(\theta)$[19]

$$\mathbf{S}(\theta)=\begin{bmatrix} S_{11} & S_{12} & 0 & 0 \\ S_{12} & S_{22} & 0 & 0 \\ 0 & 0 & S_{33} & S_{34} \\ 0 & 0 & -S_{34} & S_{44} \end{bmatrix}, \quad (3)$$

where $0^\circ \leqslant \theta \leqslant 180^\circ$ is the scattering angle. The scattering matrix element $S_{11}$ is traditionally called the phase function and satisfies the following normalization condition,

$$\frac{1}{2}\int_0^\pi \sin\theta S_{11}(\theta)\mathrm{d}\theta = 1 \ . \quad (4)$$

Another useful quantities are the orientation-averaged absorption cross-section, $C_{\rm abs} = C_{\rm ext} - C_{\rm sca}$, the single-scattering albedo, $\omega = C_{\rm sca}/C_{\rm ext}$, and the asymmetry parameter defined by

$$g \equiv \langle\cos\theta\rangle = \frac{1}{2}\int_0^\pi S_{11}(\theta)\sin\theta\cos\theta\mathrm{d}\theta \ . \quad (5)$$

For randomly-oriented aggregates, the optical characteristics are given as

$$< Q >= \frac{1}{8\pi^2}\int_0^{2\pi}\int_{-1}^{1}\int_0^{2\pi} Q(\beta,\Theta,\Phi)\mathrm{d}\beta\mathrm{d}(\cos\Theta)\mathrm{d}\Phi \ , \quad (6)$$

where Euler angles $\beta, \Theta$, and $\Phi$ specify the particle's orientation with respect to the laboratory reference frame. For a randomly-oriented target with no symmetry, the Euler angles $\beta \in [0, 2\pi)\,, \Theta \in [0, \pi)\,$, and $\Phi \in [0, 2\pi)$. We use tuple $(n_\beta, n_\Theta, n_\Phi)$ to denote that there are $n_\beta$ angles chosen for $\beta$, $n_\Theta$ for $\Theta$, and $n_\Phi$ for $\Phi$. In this study, $n_\beta = 10, n_\Theta = 7$, and $n_\Phi = 7$ , i.e., 490 orientations are considered in the determination of the orientationally averaged values of all the scattering matrix elements and optical cross-sections .The number of orientations required in the calculations for the randomly-oriented aggregates are enough[20].

As demonstrated in Ref. [21], soot clusters may tend to aggregate with ammonium sulfate, dust or other aerosol particles, as shown in Fig. 1. In the following, we will describe and analyze the scattering and absorption properties of such complex aerosols. Once again, the cluster-generation code developed by Lei *et al.*[22] was used to simulate a soot cluster. We fixed the fractal prefactor at 5.8, the fractal dimension at 1.8[10], and the number of monomers in each soot cluster was fixed at 100. After a soot cluster was generated, it was randomly attached to a larger aerosol particle, thereby resulting in a specific realization of a chemically heterogeneous aggregate. In this study, all computations of light scattering and absorption by complex soot aggregates have been performed at a fixed visible wavelength of 0.628 $\mu$m.

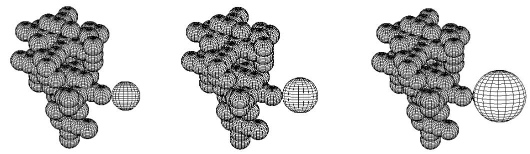

Fig. 1. Aggregates formed by fractal soot clusters ($D_{\rm f} = 1.8$, $K_{\rm f} = 5.8$, $N = 100$, $a = 0.02$ $\mu$m) attached to a larger aerosol particle (soot, ammonium sulfate, dust or other aerosol particle) with different sizes.

Table 1 summarizes the orientation-averaged integral photometric characteristics of the complex aerosols formed by aggregation of soot clusters with a larger particle. The soot monomer radius is 0.02 $\mu$m, and the soot refractive index is 1.75+i0.435 at 0.628 $\mu$m[23]. The radius of larger particle is from 0.02 to 0.3 $\mu$m, and can be either an ammonium sulfate, or dust particle with the respective refractive index 1.44 or 1.53+i0.008[24]. In Table 1 the relative deviation $\sigma$ is defined as

$$\sigma = \left|\frac{C_1 - C_2}{C_1}\right|, \quad (7)$$

where $C_1$ and $C_2$ are the results calculated for the soot clusters with a larger particle (soot-soot, soot-sulfate, or soot-dust aggregates) and the single larger particle, respectively. As shown in Table1, the orientation-averaged extinction $C_{\rm ext}$, scattering $C_{\rm sca}$, and absorption $C_{\rm abs}$, cross-sections, the single-scattering albedo, and the asymmetry parameter are all gradually increased, and the relative deviations of the radiative properties rapidly decrease with the increasing of the radius of larger particle. This indicate that the size of the larger particle has a pronounced effect on the overall radiative properties of the aggregates, i.e., the larger particle dominates the overall radiative properties of the complex aggregates. Furthermore, the material composition of the larger particle has a very significant effect on the radiative properties of the aggregates.

Figure 2 depicts the scattering matrix elements of a soot-soot aggregate in random orientation. The radia of the larger particle are 0.05 and 0.1 $\mu$m. The angular scattering characteristics calculated for the soot-sulfate,

**Table 1. Radiative Properties of Soot-soot Aggregates**

| r ($\mu$m) | $C_{\rm ext}$ ($\mu$m$^2$) | $C_{\rm abs}$ ($\mu$m$^2$) | $C_{\rm sca}$ ($\mu$m$^2$) | $\omega$ | $g$ | $\sigma_{\rm ext}$ | $\sigma_{\rm abs}$ | $\sigma_{\rm sca}$ | $\sigma_\omega$ | $\sigma_{\rm g}$ |
|---|---|---|---|---|---|---|---|---|---|---|
| 0.02 | 0.02501 | 0.02073 | 0.00428 | 0.1710 | 0.5213 | 0.9927 | 0.9912 | 0.9997 | 0.9613 | 0.9833 |
| 0.05 | 0.02887 | 0.02385 | 0.00502 | 0.1738 | 0.5431 | 0.8766 | 0.8633 | 0.9396 | 0.5109 | 0.9004 |
| 0.10 | 0.07382 | 0.05167 | 0.02213 | 0.2997 | 0.5748 | 0.3648 | 0.3876 | 0.3117 | 0.0837 | 0.5780 |
| 0.20 | 0.38791 | 0.20675 | 0.18117 | 0.4671 | 0.6826 | 0.0643 | 0.0828 | 0.0433 | 0.0225 | 0.0184 |
| 0.25 | 0.60485 | 0.31441 | 0.29044 | 0.4802 | 0.7421 | 0.0373 | 0.0509 | 0.0225 | 0.0153 | 0.0077 |
| 0.30 | 0.82713 | 0.44459 | 0.40055 | 0.4843 | 0.7825 | 0.0202 | 0.0326 | 0.0129 | 0.0074 | 0.0038 |

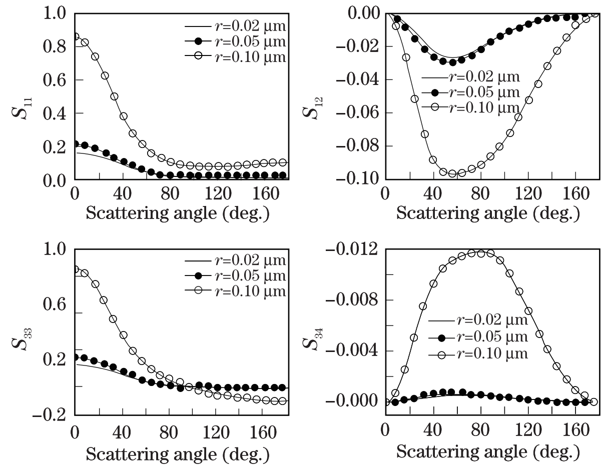


Fig. 2. Orientation-averaged scattering matrix elements versus scattering angle for aerosols formed by aggregation of soot clusters with a larger soot particle.

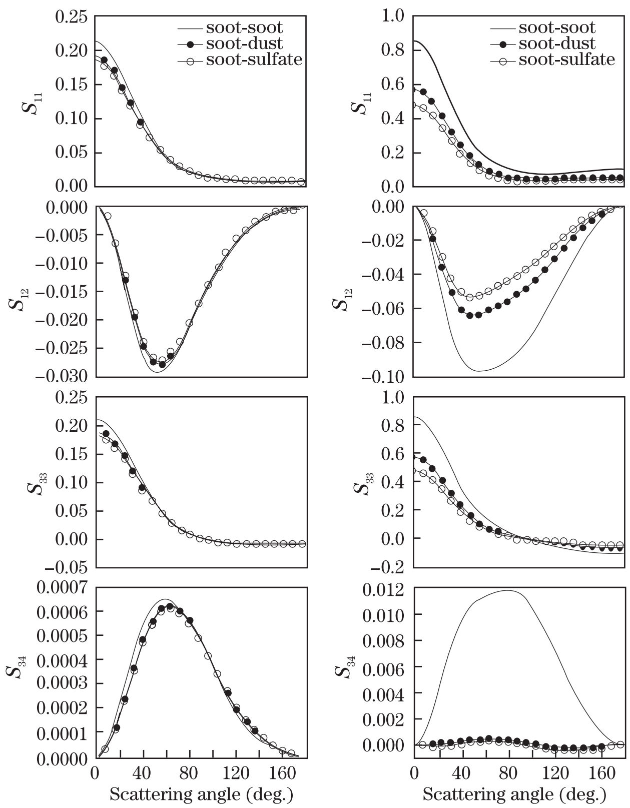


Fig. 3. Orientation-averaged scattering matrix elements versus scattering angle for aerosols formed by aggregation of soot clusters with a larger particle with different chemical components.

soot-dust aggregates are rather similar except for magnitude and are not discussed specifically. It is quite obvious that larger particle contributes considerably to total scattering matrix elements of the complex aggregates, larger particle dominates cumulative scattering matrix. The total phase function $S_{11}$ is strongly forward-directed, which is typical of wavelength-sized scatterers. With the increase of the radius of larger particle, the value of $S_{11}$ increases rapidly, especially at the forward-scattering direction, and $S_{33}$ increases at smaller scattering angles, but decreases at large scattering angles. The values of $S_{12}$ and $S_{34}$ decrease or increase rapidly at side-scattering angles as the radius of larger particle increase.

Figure 3 illustrates the differences in the scattering matrix elements between the soot-soot, soot-dust, and soot-sulfate aggregates. The radia of the larger particles are 0.05 $\mu$m (left panels) and 0.1 $\mu$m (right panels), respectively. As shown in Fig. 3, the chemical component of the larger particle has a strong effect on the total scattering matrix elements of the complex aggregates, and the effect will become stronger with the increase of the radius of the larger particle.

In conclusion, we analyze the effects of the material composition and the size of the larger particle that is in touch with a soot cluster on scattering and radiative properties of complex soot aggregates. Our numerical results show that the material composition and the size of the larger particle can strongly influence, or even dominate, the overall light-scattering and radiative properties of the aggregates. The larger particle can absolutely dominate the overall scattering and radiative properties of complex soot aggregates.

We thank Professor Draine for providing the DDA codes.

## References


1. C. M. Sorensen, Aerosol Sci. Technol. **35,** 648 (2001).
2. M. I. Mishchenko, B. Caims, J. E. Hansen, L. D. Travis, R. Burg, Y. J. Kaufman, J. V. Martins, and E. P. Shettle, J. Quant. Spectrosc. Radiat. Transfer **88,** 149 (2004).
3. M. Z. Jacobson, Nature **409,** 695 (2001).
4. S. Menon, J. Hansen, L. Nazarenko, and Y. Luo, Science **297,** 2250 (2002).
5. A. Ben-David, J. F. Embury, and C. E. Davidson, Appl. Opt. **45,** 6860 (2006).
6. K. N. Liou, Y. Gu, W. L. Lee, Y. Chen, and P. Yang, *Some Unsolved Problems in Atmospheric Radiative Transfer: Implication for Climate Research in the Asia-Pacific Region* (World Scientific Publishing Co., Singapore, 2009).
7. R. Y. Zhang, A. F. Khalizov, J. Pagels, D. Zhang, H. X. Xue, and P. H. Mcmurry, Proc. Nat. Acad. Sci. USA **105,** 10291 (2008).
8. J. Haywood and O. Boucher, Rev. Geophys. **38,** 513 (2000).
9. S. J. Abel, J. M. Haywood, E. J. Highwood, J. Li, and P. R. Buseck, Geophys. Res. Lett. **30,** 1783 (2003).
10. C. Lei, H. Zhang, and H. Liu, Acta Phys. Sin. (in Chinese) **58,** 7168 (2009).
11. C. Lei and Z. Wu, Acta Phys. Sin. (in Chinese) **59,** 5692 (2010).
12. C. Lei, H. Liu, and H. Zhang, Acta Opt. Sin. (in Chinese) **30,** 876 (2010).
13. A. V. Filippov, M. Zurita, and D. E. Rosner, J. Colloid Interface Sci. **229,** 261 (2000).
14. D. W. Mackowski, J. Quant. Spectrosc. Radiat. Transfer **100,** 237 (2006).
15. E. M. Purcell and C. R. Pennypacker, Astrophys. J. **186,** 705 (1973).
16. B. T. Draine, Astrophys J. **333,** 848 (1988).
17. B. T. Draine and J. J. Goodman, Astrophys. J. **405,** 685 (1993).

18. B. T. Draine and P. J. Flatau, J. Opt. Sci. Am A **11,** 1491 (1994).
19. M. I. Mishchenko and L. D. Travis, *Scattering, Absorption, and Emission of Light by Small Particles* (Cambridge University Press, Cambridge, 2002).
20. S. Manickavasagam and M. P. Mengüc, Appl. Opt. **36,** 1337 (1997).
21. J. Li, J. R. Anderson, and P. R. Buseck, J. Geophys. Res. **108,** 4189 (2003).
22. C. Lei and Z. Wu, Chin. J. Comput. Phys. (in Chinese) **27,** 593 (2010).
23. J. S. Wu, S. S. Krishnan, and G. M. Faeth, ASME J. Heat Transfer **119,** 230 (1997).
24. G. A. d'Almeida, P. Koepke, and E. P. Shettle, *Atmospheric Aerosols*: *Global Climatology and Radiative Characteristics* (Deepak Press, Virginia, 1991).